ISBN: 978-3-95450-132-8 doi:10.18429/JACoW-IPAC2014-MOPRO055

ESRF UPGRADE PHASE II STATUS

J-L. Revol, P. Berkvens, J-C. Biasci, J-F. Bouteille, N. Carmignani, J. Chavanne, F. Ewald, L. Farvacque, L. Goirand, M. Hahn, L. Hardy, J. Jacob, J-M. Koch, G. Le Bec, S. Liuzzo, T. Marchial, D. Martin, B. Nash, T. Perron, E. Plouviez, P. Raimondi, K. Scheidt, V. Serrière, R. Versteegen, ESRF, Grenoble, France

Abstract

The ESRF is close to the end of the first phase (2009-2015) of its Upgrade Programme and has defined the objectives for the ensuing second phase. It envisions a major upgrade of the source to best serve the new science opportunities. The ESRF Council endorsed the proposal to perform the technical design study of a new 7-bend achromat lattice. This configuration will allow the storage ring to operate with a decrease in horizontal emittance by a factor of about 30 and a consequent increase in brilliance and coherence of the photon beam. This paper reports on the status of the accelerator project, highlighting the progress in the technical design.

ESRF UPGRADE PROGRAMME

The European Synchrotron Radiation Facility (ESRF) is a user research facility located in Grenoble, France, supported and shared by 19 countries. Researchers, from both academia and industry, exploit 42 highly specialised beamlines, the intense X-rays beams produced by the 6 GeV electrons circulating in the storage ring.

In 2009, after 15 years (1994-2009) of successful user operation, the ESRF launched an ambitious Upgrade Programme aiming to address new scientific challenges. The first phase (2009-2015), focused on new and improved beamlines and instrumentation, is close to completion. The second phase proposes the design and implementation of a new low emittance lattice storage ring to be constructed and commissioned in the existing storage ring tunnel in place of the present one [1]. This challenging project [2] will be carried out in the period 2015-2020, to be followed in the period 2020-2022 by the construction of four new state-of-the-art beamlines.

STORAGE RING LATTICE DESIGN

The equilibrium emittance of the electron storage ring will be minimised by increasing the number of bending magnets and accommodating strong quadrupoles that provide the necessary focusing between the dipoles [3]. The lattice has been optimised to achieve the minimum emittance with the following constraints:

- Straight section long enough to accommodate the present low-gap, 5 m-long, insertion device vacuum chambers.
- Quadrupole strengths compatible with state-of-the-art magnet and vacuum chamber designs.
- Drift space between magnets optimized to accommodate the vacuum system, the absorbers and allowing the integration of the diagnostics.

The lattice comprises 30 identical standard cells and two special cells that provide a special straight section for injection. The optical functions are the same in all standard straight sections, thus disposing of the alternating high and low-beta straight sections of the present lattice. Figure 1 shows the optical functions of a standard cell. The main parameters are listed in Table 1.

The equilibrium emittance reaches 147 pm•rad. With a set of insertion devices giving an energy loss of 0.47 MeV, which is the present average value, the emittance delivered in user service mode will be below 120 pm•rad. The target vertical emittance is set to 5 pm•rad, corresponding to a coupling value of 3.5%.

The insertion device source points will be kept the same as in the present lattice. This implies a reduction of the ring circumference of about 0.41m and a corresponding increase of the RF frequency by 171 kHz. The booster circumference will have to be reduced accordingly.

Table 1: Lattice Parameters

Lattice	Present	New
Lattice type	DBA	HMBA
Circumference [m]	844.390	843.979
Beam energy [GeV]	6.04	6.00
Natural emittance [pm•rad]	4000	147
Vertical emittance [pm•rad]	4	5
Energy spread [%]	0.106	0.095
Damping times H/V/L [ms]	7/7/3.5	8.5/13/8.8
Energy loss /turn [MeV]	4.88	2.60
Tunes (H/V)	36.44/ 13.39	75.58/ 27.62
Chromaticity (H/V)	-130/-58	-100/-84
Momentum compaction	$1.78\ 10^{-4}$	$0.87\ 10^{-4}$

The non-linear optimisation involves two sextupole families per cell, located in the high-dispersion regions to correct the horizontal and vertical chromaticities. The phase advances between the sextupoles at both ends of the cell are set to 3π in the horizontal plane and π in the vertical, yielding a minus identity transform between the sextupoles. This property cancels most of the undesirable effects of the sextupoles. This setup provides a satisfying dynamic aperture without any need for additional sextupole families. However, since the horizontal and

ISBN: 978-3-95450-132-8 doi:10.18429/JACoW-IPAC2014-MOPRO055

vertical sextupoles are interleaved, they still generate large amplitude-dependent tune shifts. These are minimised by a combination of a slight deviation from the exact π phase advance and the introduction of two families of octupoles.

As the horizontal beta-function in the standard straight section is only 5.2 m, a special injection section has been designed with β_x=18.4m at the septum. Symmetry breaking is limited because the phase advance in each plane is identical to the standard cell ones, as well as the optical functions across the sextupoles. On both sides of the injection straight section, 430 mm of space is available for two kickers, allowing an injection scheme similar to the present one. As there is no sextupole within the injection kicker bump, there will be no perturbation of the circulating beam when powering the injection bump, ensuring a stable beam in top-up operation.

In order to optimise the magnets and the vacuum system engineering, three beam stay-clear regions have been considered. In the central part, the beta functions are small and consequently the beam stay-clear could be reduced (Table 2), making the magnet design easier in order to reach the required high gradients. Similarly, in the insertion device region, the vertical beta is compatible with the smallest possible vertical gap of the undulators.

The present lattice design already closely matches the engineering requirements.

Table 2: Beam Stay-Clear Specification

	Horizontal	Vertical
Centre	±15mm	±6.5 mm
Up and downstream	±25 mm	±10 mm
Insertion device straight	±15 mm	±2.0 mm

X-RAY SOURCES

The new lattice will provide an improvement in brightness of the order of 30-100 times for both insertion device and bending magnet beamlines (Figure 2). The coherence fraction on insertion device beamlines will also increase by up to a factor of 30. Since the X-ray beam will be much narrower, it will be possible to collimate a larger fraction of the white beam component compared to the present. This will result in a reduction of the total power in a defined aperture; on high-beta beamline optics by more than a factor of two and on the low-beta optics by up to a factor of 10. The geometry of the insertion device beamlines will be unchanged; the beam parameters at the source result in tolerable changes in power density on the beamline optics.

Since the dipole fields will have become much weaker, the source for the bending magnet beamlines will be replaced by three-pole wigglers, resulting in an increase in brightness and flexibility of the X-ray spectra.

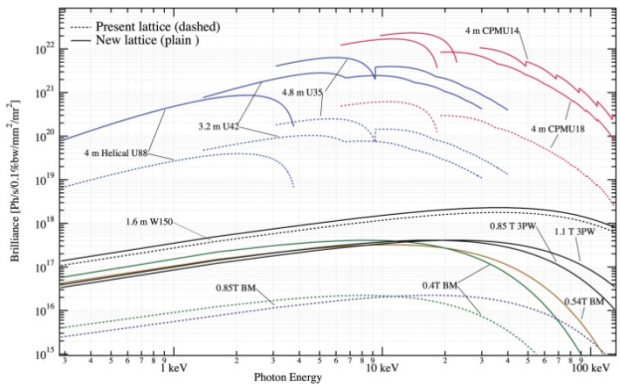

Figure 2: Brilliance from various sources for the existing and new lattices.

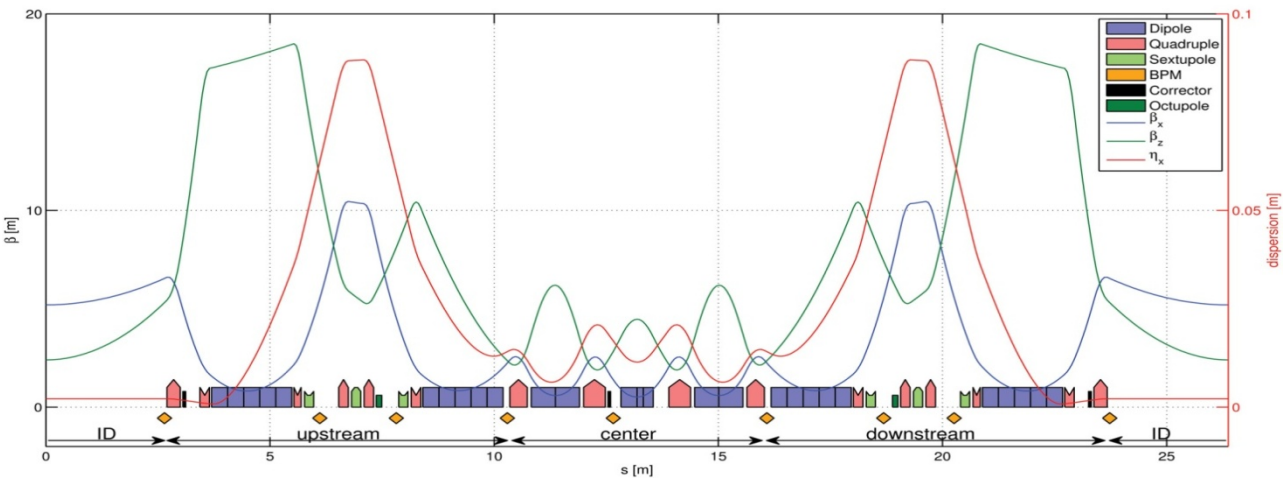

Figure 1: Optical functions of a standard cell of the hybrid multi-bend achromat lattice (HMBA). The space left between dipoles 1 and 2, and 6 and 7 allows the beta-functions and dispersion to grow to high values, making the sextupoles more efficient. In the central part, four high-gradient horizontally-focusing quadrupoles and three high-gradient bending magnets, which also provide vertical focusing, are alternately placed. At each end of the cell, two dipoles encompass the regions with large beta-functions and dispersion. Their longitudinally varying bending field helps to reduce the emittance and to increase the dispersion.

ISBN: 978-3-95450-132-8 doi:10.18429/JACoW-IPAC2014-MOPRO055

ENGINEERING DESIGN

The design benefits as much as possible from standard technology and expertise gained at the ESRF and similar facilities. The necessary prototyping has been made compatible with the project timescale and the validation process.

Magnets

The design of the magnets of the new storage ring is challenging, with magnetic specifications exceeding those of the present third-generation light sources. More than 1000 magnets (Table 3), including new concepts such as dipoles with longitudinal gradients, must be ready for installation in 2018, leading to short development time [4]. The magnet designs are relatively conventional for quadrupoles and sextupoles, but the large gradients required has led to bore radii reduced by a factor of three, compared to the magnets of the present storage ring. This has had an impact on the field quality, on the tolerances, and finally on the mechanical design. Dipoles with a longitudinal field gradient are new magnets, and various designs have been envisaged, including permanent magnets. Moreover, an effort has been made towards compact design and to reduce the power consumption of all the magnets. All magnets will be powered individually, in contrast to connection by family for the present lattice.

Table 3: Magnet Strengths and Quantity

	Quantity	Strength
Dipoles	128	0.17–0.67 T
Dipole quadrupoles	96	0.43–0.54 T 34 T/m
Quadrupoles	384	52 T/m
	128	85 T/m
Sextupoles	192	900–2200 T/m^2
Octupoles	64	51.2 10^3 T/m^3
Correctors H(V)	96	0.08 Tm

Vacuum System

A conservative approach has been chosen for the vacuum system layout [5]. Vacuum chambers with an antichamber will provide space and access for discrete ultra-high vacuum pumps and lumped absorbers. The limited available space restricts the locations where vacuum chamber hardware such as flanges, bellows, pumps and diagnostic equipment can be installed. The design and distribution of vacuum chambers is therefore more complex than in the present storage ring. In addition, the vacuum chamber distribution should facilitate the preparation of pre-assembled girders with magnets, vacuum chambers and vacuum equipment.

Lump absorbers, crotch absorbers and a few special absorbers protect the vacuum chambers from the synchrotron radiation power generated by the dipoles. All the absorbers will be made of oxygen-free high thermal conductivity (OFHC) copper and will be water-cooled, and with no water-to-vacuum joint. The insertion device chambers consist of the 5 m aluminium extruded profile NEG-coated vacuum chambers already installed and conditioned in the existing storage ring. To further decrease the average vacuum pressure and the gas-bremsstrahlung in the straight section, the two chambers on each side of the straight section chambers will be NEG coated as well.

Radio Frequency

The new RF system is dimensioned for 6 MV, providing 4.9% of RF energy acceptance. In order to push the longitudinal coupled bunch instability threshold, the project will benefit from the single-cell HOM-damped cavities developed during Phase I. The RF system will be perfectly matched at 200 mA with 14 cavities in operation, requiring 890 kW of RF power produced by a mix of the existing solid state amplifiers and klystrons. A straight section of the new lattice provides enough space for five HOM damped cavities, the necessary tapers, bellows and photon absorbers, as well as vacuum valves.

IMPLEMENTATION

The green light for the execution of the project is expected to be given in autumn 2014.

The accelerator project will be carried out while maintaining operational performances of the facility.

The technical and engineering design is ongoing and will allow the procurement phase to be started from 2015 onwards. The pre-assembly phase will take place during 2017-2018. The dismantling of the present storage ring and the installation of the new storage ring (Fig. 3) is planned to start on the 15 October 2018 for a total duration of nine months, followed by a commissioning period for the new accelerator and the beamlines. The user service mode is expected to resume in June 2020.

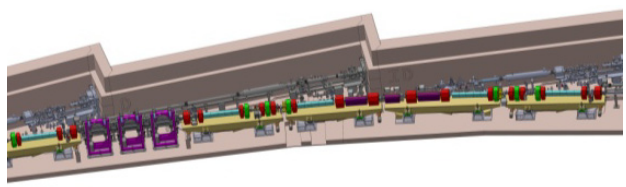

Figure 3: 3D layout.

REFERENCES

[1] J.-L. Revol et al., "ESRF Upgrade Phase II," IPAC2013, TUOAB203, Shanghai, China.
[2] http://www.esrf.fr/cms/live/live/en/sites/www/home/about/upgrade.html
[3] L. Farvacque et al., "A Low-emittance Lattice for the ESRF", IPAC2013, MOPEA008, Shanghai, China.
[4] G. Le Bec et al., "Shape Optimization for the ESRF II Magnets", TUPRO082, these proceedings, IPAC2014.

ISBN: 978-3-95450-132-8 doi:10.18429/JACoW-IPAC2014-MOPRO055

[5] M. Hahn et al., "Layout of the Vacuum System for a New ESRF Storage Ring", WEPME026, these proceedings, IPAC2014.